Baseline SUV_{max} is related to tumor cell proliferation and patient outcome in follicular lymphoma

Cédric Rossi,[1-5] Marie Tosolini,[1,3,6,7] Pauline Gravelle,[1-4,6] Sarah Pericart,[1,6] Salim Kanoun,[8] Solene Evrard,[6] Julia Gilhodes,[9] Don-Marc Franchini,[1-4] Nadia Amara,[6] Charlotte Syrykh,[6, 10,11] Pierre Bories,[10,11] Lucie Oberic,[11] Loïc Ysebaert,[1-4,11] Laurent Martin,[12,13] Selim Ramla,[12,13] Philippine Robert,[5,13] Claire Tabouret-Viaud,[14] René-Olivier Casasnovas,[5,13] Jean-Jacques Fournié,[1-4] Christine Bezombes[1-4#] and Camille Laurent[1-4,6#]

[1]Centre de Recherches en Cancérologie de Toulouse (CRCT), UMR1037 INSERM, Université Toulouse III Paul-Sabatier, ERL5294 CNRS, Toulouse; [2]Laboratoire d'Excellence TOUCAN, Toulouse; [3]Programme Hospitalo-Universitaire en Cancérologie CAPTOR, Université Toulouse, Toulouse; [4]CALYM Carnot Institute, Pierre-Bénite; [5]CHU Dijon, Hématologie Clinique, Hôpital François Mitterrand, Dijon; [6]Département de Pathologie, Institut Universitaire du Cancer de Toulouse, Université Toulouse, Toulouse; [7]Pôle Technologique du Centre de Recherches en Cancérologie de Toulouse, Toulouse; [8]Médecine Nucléaire, Institut Universitaire du Cancer Toulouse-Oncopole, Université Toulouse, Toulouse; [9]Bureau des Essais Cliniques, Institut Universitaire du Cancer Toulouse-Oncopole, Université Toulouse, Toulouse; [10]Réseau Régional de Cancérologie, Onco-Occitanie, Institut Universitaire du Cancer, Université Toulouse, Toulouse-Oncopole; [11]Service d'Hématologie, Institut Universitaire du Cancer de Toulouse, Université Toulouse Toulouse; [12]Département de Pathologie, CHU Hôpital François Mitterrand, Dijon; [13]INSERM UMR 1231 UFR, Bourgogne and [14]Département de Médecine Nucléaire, Centre Georges-François Leclerc, Dijon, France

[#]CB and CL contributed equally as co-senior authors.

©2022 Ferrata Storti Foundation. This is an open-access paper. doi:10.3324/haematol.2020.263194

Received: June 24, 2020.

Accepted: December 11, 2020.

Pre-published: December 17, 2020.

Correspondence: *CHRISTINE BEZOMBES* - christine.bezombes@inserm.fr

CAMILLE LAURENT - laurent.camille@iuct-oncopole.fr

CÉDRIC ROSSI - cedric.rossi@chu-dijon.fr

Title: Baseline SUVmax is related to tumor cell proliferation and patient outcome in follicular lymphoma

Rossi C et al.

Supplemental Data

Table of contents:

Supplemental Methods

PET/CT acquisition and analysis

Baseline PET acquisition was performed before any treatment using two types of scanners: GE Healtcare Discovery IQ and Philips Gemini TF16, with VPHD-S and BLOB-OS-TF reconstruction algorithms, respectively. The median time interval between FDG injection and image acquisition was 65 minutes (ranging from 55 to 74 minutes) with no difference between the two clinical centers.

Patients were instructed to fast for at least 6 hours before the injection of 250 to 550 MBq of 18FDG (>3MBq/kg). Measures of blood glucose level prior to FDG injection and after 4h of fasting were collected in 118 FL patients (n=118/132 patients with available data). The upper level of serum glucose permitted before patient scanning was 11mmol/l. The mean fasting plasma glucose level was 5.88 mmol/l (ranging from 3.7 to 10.22 mmol/l).

Patients were asked to avoid physical exercise 24 hours before PET acquisition, in order to avoid diffuse muscular FDG uptake. A whole-body acquisition with a full-ring dedicated PET camera and attenuation correction was started 60 minutes after the FDG injection, from head to mid-thigh. The acquisition time was at least 2 minutes per bed position. Images were reconstructed using an iterative algorithm. The image voxel counts were calibrated to activity concentration (Bq/mL) and converted into SUV with decay-correction using the time of tracer injection as a reference.

Histopathology and immunohistochemistry studies

Three-µm-thick sections of available formalin-fixed-paraffin-embedded (FFPE) FL lymph node samples (n=38/48 from the training cohort and n=41/84 from the validation cohort) were tested using Ventana Benchmark XT immunostainer (Ventana, Tucson, AZ). Samples from the training cohort were stained with PD-1 (clone NAT-105; Ventana Medical Systems), TIM3 (goat polyclonal; R&D), PD-L1 (Clone E1L3N, Cell Signaling Technologies), LAG3 (rabbit polyclonal; Novus Biologicals), CD8 (clone SP57, Ventana Medical Systems), CD3 (clone 2GV6, Ventana Medical Systems) and CD163 (10D6; Novocastra). Staining of Ki-67 (clone MIB-1, Dako) was done in the training and validation cohorts.) The IHC slides were digitalized using Panoramic 250 Flash II digital microscopes (3DHISTECH, Budapest, Hungary). IHC staining was scored by three pathologist (SP, CL and LM) and by an automated method using a computer assisted software (Tissue Studio, Definiens, Munich, Germany).[1] For automated quantification, digital images were annotated by a pathologist to denote tumor region of interest containing follicles and interfollicular areas, and the nuclei were detected and segmented according to their content of hematoxylin and chromogen (DAB). A machine learning algorithm was then trained to filter and discard false positive or negative artifacts. A classifier was applied to count the number of

nuclei positive for Ki67 antibody (staining in purple) and negative for Ki67 antibody (uncolored nuclei) in each sample.

Data mining and transcriptome analyses

Raw data were normalized together using RMA methods and collapsed to HUGO gene symbols using chipset definition files available from the NCBI gene expression omnibus. The RMA (robust multi-array average)-normalized expression data were scored using the AutocompareSES software (available at https://sites.google.com/site/fredsoftwares/products/autocompare_ses) using the "greater" (indicating an enriched gene set) Wilcoxon tests with frequency-corrected null hypotheses and normalized setting. Gene Sets used were the immune escape gene set 33 (IEGS33).[2] Public raw data of FL transcriptomes were downloaded from the NCBI-GEO data set repository (GSE53820[3], GSE55267[4], GSE65135[5], GSE16024[6], GSE16455[7], GSE21554[8]), normalized together and collapsed to HUGO gene symbols using chipset definition files available from the NCBI gene expression omnibus. Gene sets from Gene Ontology[9] and/or GO Consortium and reactome [9,10] were downloaded and used in the AutoCompare-SES software. To correct platform effect on IEGS33 and T cell activation sample enrichment scores (SES), lymphocytes samples from GSE62923, GSE28726 and GSE39594[11–13] were used as controls. Assessments of leucocyte fractions from the specified transcriptomes were performed using CIBERSORT (https://cibersort.stanford.edu/) with 500 Monte Carlo iterations and the LM7 matrix.

Abundances were calculated from the CIBERSORT results and the SES using the open source software DeepTIL (https://sites.google.com/site/fredsoftwares/products/deeptil). This software was used to automatically compute the abundance of the seven leucocyte subsets in the samples as previously described.

Mutation profile analysis with next-generation sequencing

Tumor DNA was extracted from 10 µm-thick sections of 51 available FL FFPE (n=33 from training cohort and n=18 from validation cohort) using Qiagen QIAamp DNA FFPE Tissue Kit (Qiagen Inc., Valencia, CA) according to the manufacturers' recommendations. The lymphopanel was designed to identify mutations in 43 genes involved in B cell lymphomagenesis.[14] Samples were prepared following the TSCA protocol.[15] Multiple indexed libraries were pooled and sequenced on the Illumina NextSeq using a mid-output flowcell with 300X average depth. After pair-end sequencing (2x150 cycles), the four FastQ files generated were analyzed using Amplicon DS (v1.1.13.0, Illumina).[14] After variant calling, variants detected by AmpliconDS software were filtered regarding their consequence as described previously.[14]

References

1. Péricart S, Tosolini M, Gravelle P, et al. Profiling Immune Escape in Hodgkin's and Diffuse large B-Cell Lymphomas Using the Transcriptome and Immunostaining. Cancers 2018;10(11):415.

2. Tosolini M, Algans C, Pont F, Ycart B, Fournié J-J. Large-scale microarray profiling reveals four stages of immune escape in non-Hodgkin lymphomas. Oncoimmunology 2016;5(7):e1188246.

3. Brodtkorb M, Lingjærde OC, Huse K, et al. Whole-genome integrative analysis reveals expression signatures predicting transformation in follicular lymphoma. Blood 2014;123(7):1051–1054.

4. Guo S, Chan JKC, Iqbal J, et al. EZH2 mutations in follicular lymphoma from different ethnic groups and associated gene expression alterations. Clin Cancer Res Off J Am Assoc Cancer Res 2014;20(12):3078–3086.

5. Newman AM, Liu CL, Green MR, et al. Robust enumeration of cell subsets from tissue expression profiles. Nat Methods 2015;12(5):453–457.

6. Fernàndez V, Salamero O, Espinet B, et al. Genomic and gene expression profiling defines indolent forms of mantle cell lymphoma. Cancer Res 2010;70(4):1408–1418.

7. Watkins AJ, Hamoudi RA, Zeng N, et al. An integrated genomic and expression analysis of 7q deletion in splenic marginal zone lymphoma. PloS One 2012;7(9):e44997.

8. Ashburner M, Ball CA, Blake JA, et al. Gene ontology: tool for the unification of biology. The Gene Ontology Consortium. Nat Genet 2000;25(1):25–29.

9. Fabregat A, Sidiropoulos K, Garapati P, et al. The Reactome pathway Knowledgebase. Nucleic Acids Res 2016;44(D1):D481-487.

10. Milacic M, Haw R, Rothfels K, et al. Annotating cancer variants and anti-cancer therapeutics in reactome. Cancers 2012;4(4):1180–1211.

11. Constantinides MG, Picard D, Savage AK, Bendelac A. A naive-like population of human CD1d-restricted T cells expressing intermediate levels of promyelocytic leukemia zinc finger. J Immunol Baltim Md 1950 2011;187(1):309–315.

12. Whisenant TC, Peralta ER, Aarreberg LD, et al. The Activation-Induced Assembly of an RNA/Protein Interactome Centered on the Splicing Factor U2AF2 Regulates Gene Expression in Human CD4 T Cells. PloS One 2015;10(12):e0144409.

13. Martínez-Llordella M, Esensten JH, Bailey-Bucktrout SL, et al. CD28-inducible transcription factor DEC1 is required for efficient autoreactive CD4+ T cell response. J Exp Med 2013;210(8):1603–1619.

14. Evrard SM, Péricart S, Grand D, et al. Targeted next generation sequencing reveals high mutation frequency of CREBBP, BCL2 and KMT2D in high-grade B-cell lymphoma with MYC and BCL2 and/or BCL6 rearrangements. Haematologica 2019;104(4):e154–e157.

15. Vendrell JA, Grand D, Rouquette I, et al. High-throughput detection of clinically targetable alterations using next-generation sequencing. Oncotarget 2017;8(25):40345–40358.

Supplemental Tables

Supplemental Table S1. Main clinical characteristics of follicular lymphoma patients.

Variables	All patients (n=132)	Toulouse cohort (n=48) Number of patients (%)	Dijon cohort (n=84) Number of patients (%)	*p value*
Age	Median 61.8 (28-87)	Median 62 (28-87)	Median 61.5 (33-80)	0.4
<60 years old	29 (22%) [28-59]	11 (23%) [28-58]	18 (21%) [33-59]	0.8
≥60 years old	103 (78%) [60-83]	37 (77%) [60-83]	66 (79%) [60-80]	
Sex				0.3
Female	60 (45%)	19 (39%)	41 (49%)	
Male	72 (55%)	29 (61%)	43 (51%)	
Ann Arbor Stage				0.86
I-II	21 (16%)	8 (17%)	13 (15%)	
III-IV	111(84%)	40 (83%)	71 (85%)	
ECOG Performance status				0.36
0	61 (46%)	24 (50%)	37 (44%)	
1-2	56 (42%)	21 (44%)	35 (42%)	
3-4	15 (12%)	3 (6%)	12 (14%)	
LDH concentration				0.02
>ULN	25 (19%)	14 (29%)	11 (13%)	
≤ULN	107 (81%)	34 (71%)	73 (87%)	
B2-microglobulin concentration				0.61
>ULN	78 (59%)	27 (56%)	51 (61%)	
≤ULN	54 (41%)	21 (44%)	33 (39%)	
FLIPI score				0.7
Low risk (0-1)	15 (12%)	4 (9%)	11 (13%)	
Intermediate (2)	46 (34%)	17 (35%)	29 (35%)	
High risk (≥3)	71 (54%)	27 (56%)	44 (52%)	
Histological grade				0.3
1-2	120 (91%)	42 (87%)	78 (92%)	
3A	12 (9%)	6 (13%)	6 (8%)	
Treatment				0.06
R-CHOP + Rm	109 (83%)	40 (83%)	69 (82%)	
R-CVP + Rm	8 (6%)	8 (17%)		
R-Lenalidomide + Rm (RELEVANCE)	8 (6%)		8 (10%)	
GA101-Lenalidomide + Rm (GALEN)	7 (5%)		7 (8%)	
SUV max PET baseline median (min-max)	9.15 (2.5-34.6)	10.8 (2.5-34.6)	9.5 (3.3-25.4)	0.7

Abbreviations: : R, Rituximab; CHOP, cyclophosphamide, doxorubicin, vincristine and prednisone; Rm, Rituximab maintenance; CVP, cyclophosphamide, vincristine, prednisone; ECOG, Eastern Cooperative Oncology Group; FLIPI, follicular lymphoma international prognostic index; LDH, lactic-dehydrogenase; ULN upper limit of normal.

Supplemental Table S2: Summary of main PET metrics in follicular lymphoma patients.

Parameters	SUVmax	TMTV
Median	9.15	406
Range	2.5-34.6	5-3983.9
IQR	8.95-13.85	62.6-722.5

Abbreviations: IQR: inter-quartile; SUVmax: maximum standardized uptake value; TMTV: total metabolic tumor volume.

Supplemental Table S3: List of variants detected in follicular lymphoma patients.

See Excel files uploaded separately from the pdf supplemental data files. **T**, FL patients from the training cohort; **V**, FL patients from the validation cohort.

Supplemental Figures

Supplemental Figure S1: Functional immune stages of follicular lymphoma samples from the training cohort and previously published lymphoma cohort including the PRIMA study samples.

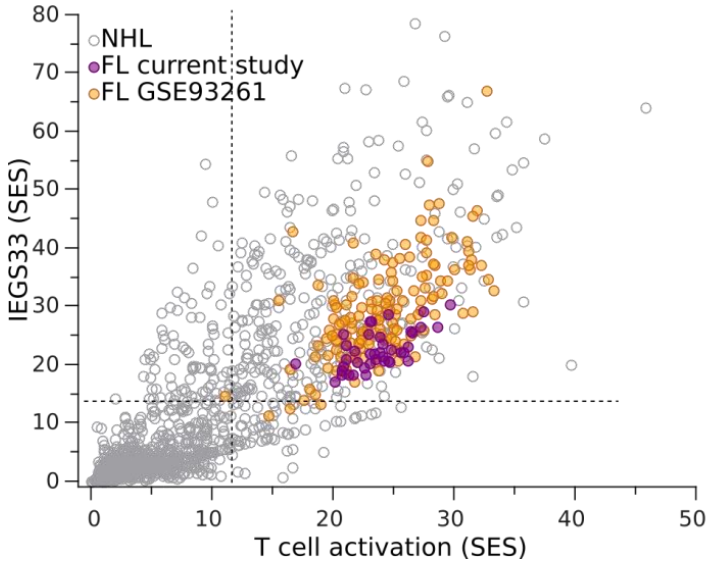

Dot plot of Sample Enrichment scores (SES) for the immune escape gene sets (IEGS33) versus T cell activation gene set (defined in14) shows clustering of follicular lymphoma (FL) samples from our training cohort (n=38 in purple dots) and from PRIMA study "GSE93261" (n=149 in orange dots) among the non-Hodgkin lymphoma public microarrays datamining analysis (n=1446 grey dots).

Supplemental Figure S2: Correlation between SUVmax and IEGS33 or SES for T cell activation from follicular lymphoma transcriptomics data of the training cohort.

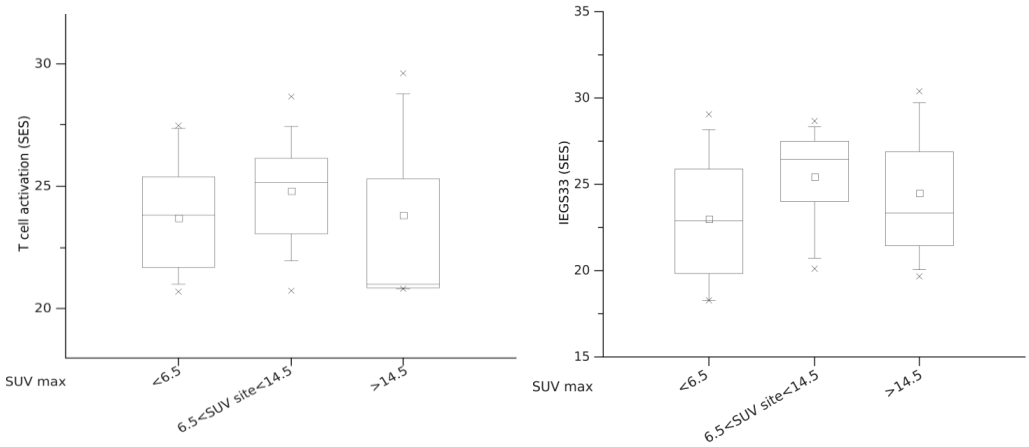

Boxplots show SES sample enrichment scores (SES) for T-cell activation and immune escape (IEGS33) of FL samples from the training cohort according to the SUVmax level at the biopsy site (SUVmax <6.5, between 6.5 and 14.5 or > 14.5).

Supplemental Figure S3: Correlation between SUVmax and deconvoluted immune cell subpopulations in the follicular lymphoma training cohort **(**using CIBERSORT deconvolution algorithm)

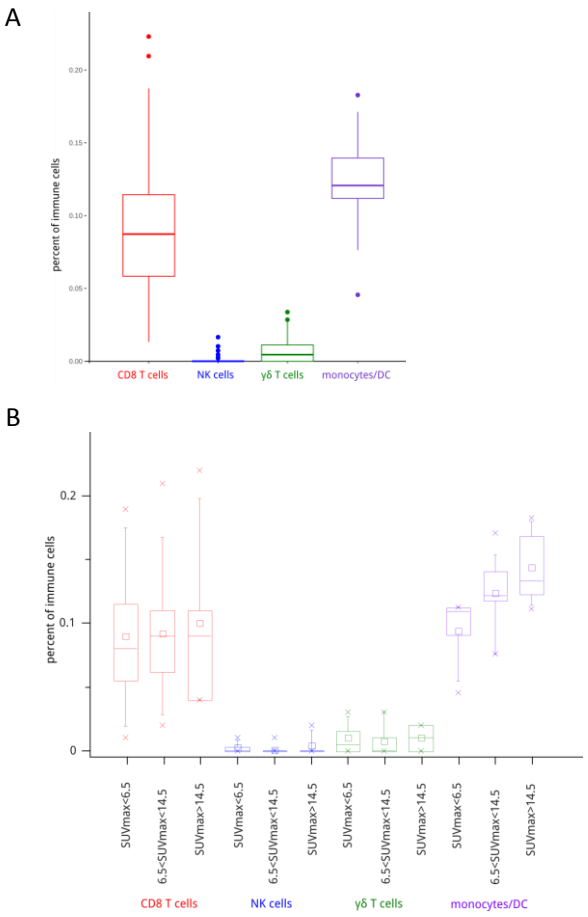

Boxplots show **(A)** Deconvoluted proportion of the four main immune cells (CD8 T cells, NK cells, γδ T cells and monocytes/dendritic cells (DC)) in FL samples of the training cohort. **(B)** Deconvoluted proportion of the four main immune cells according to the level of SUVmax. Samples were classified by their SUVmax at biopsy site (SUVmax <6.5, between 6.5 and 14.5 or > 14.5)

SUVmax Maximum Standardized Uptake value

Supplemental Figure S4: Correlation between DNA repair/tumor proliferation signatures and SUVmax in the training cohort.

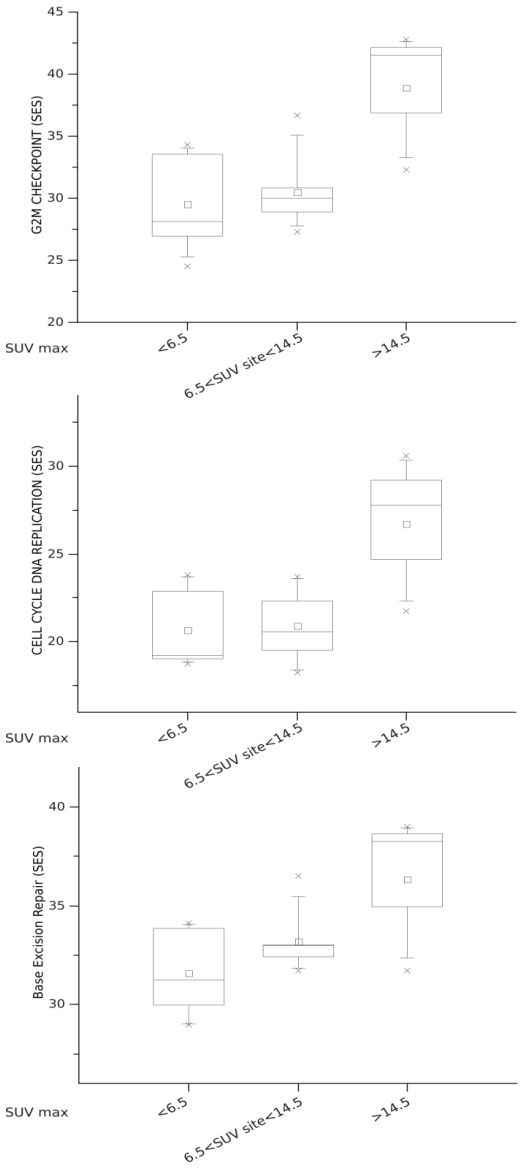

Boxplots show SES for gene signatures of G2M checkpoint, cell cycle DNA repair and Base excision repair according to the SUV max level (SUVmax <6.5, between 6.5 and 14.5 or > 14.5).

Supplemental Figure S5: Frequency of most common mutations in apoptotic and cell cycle pathways in follicular lymphoma samples according to SUVmax levels.

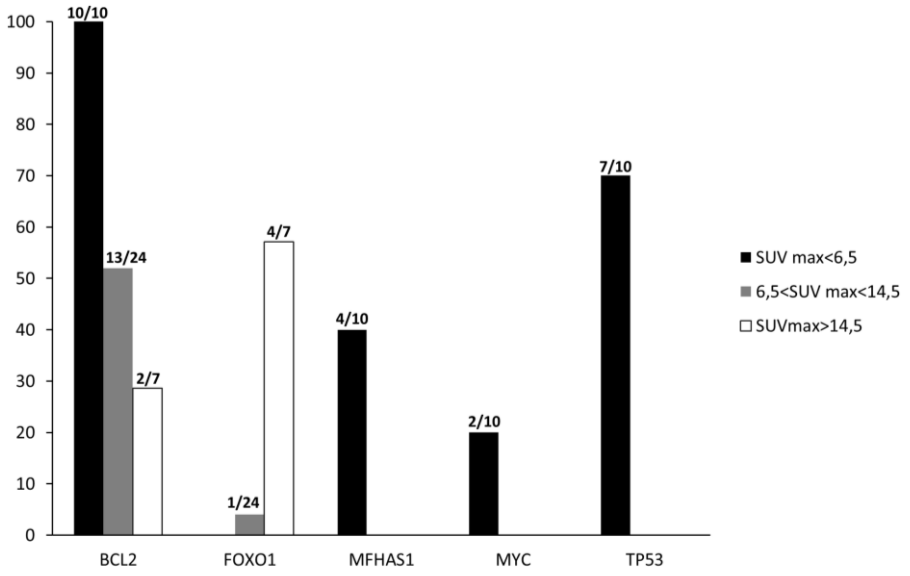

Histogram shows the distribution of *BCL2*, *FOXO1*, *MFHAS1*, *MYC* and *TP53* mutations in both FL training (n=23) and validation cohorts (n=18) according to SUVmax levels. Numbers above histogram bars correspond to the number of patients with mutation reported to the total number of patients in the SUV subgroup.